Eur. Phys. J. D (2019) 73: 137
https://doi.org/10.1140/epjd/e2019-90708-9

THE EUROPEAN PHYSICAL JOURNAL D

Regular Article

Electron impact ionisation cross sections of fluoro-substituted nucleosides*

Stefan E. Huber[a] and Andreas Mauracher[b]

Institute of Ion Physics and Applied Physics, Leopold-Franzens-University Innsbruck, Technikerstr. 25/3, 6020 Innsbruck, Austria

Received 30 December 2018 / Received in final form 25 March 2019
Published online 2 July 2019

Abstract. We report calculated electron-impact ionisation cross sections (EICSs) for 2′-deoxycytidine (*Cyt*), 2′-deoxy-5-fluorocytidine (*fCyt*) and 2′,2′-difluorocytidine (gemcitabine, *Gem*) from threshold to 10 keV. We compare the Deutsch-Märk (DM) and the binary-encounter-Bethe (BEB) methods used to obtain these cross sections. The methods yield excellent agreement with each other, within 3−4% at the cross section maxima. In particular, the DM cross sections for *Cyt*, *fCyt* and *Gem* yield maxima of 29.88 Å^2 at 79 eV, 28.96 Å^2 at 82.2 eV and 29.51 Å^2 at 83.4 eV, respectively, whereas the BEB cross sections yield maxima of 28.89 Å^2 at 87.6 eV, 27.97 Å^2 at 91.6 eV and 29.02 Å^2 at 93.4 eV, respectively. In addition, we compute EICSs for small sequences built from the considered nucleosides, i.e. for the sequences *Cyt-Cyt*, *fCyt-Cyt*, *Cyt-fCyt*, *Gem-Cyt* and *Cyt-Gem*. We find that the resulting EICSs differ only slightly between different sequences of the same constituents. Moreover, they can be approximated with an accuracy within 6% by simply adding the EICSs of individual molecular subsystems. Finally, we find that alterations in the ionisation energy due to the presence of an aqueous solvent can be substantial and may hence also considerably affect the resulting EICSs especially at low energies close to the ionisation threshold.

1 Introduction

Patients diagnosed with cancer often receive combinations of chemo- and radiotherapy in order to mutually enhance the effectiveness of the two treatments [1]. Besides cisplatin (*cis*-diamminedichloroplatinum(II)) and 5-fluorouracil, gemcitabine (2′,2′-difluorocytidine; denoted simply as *Gem* for the remainder of this work) belongs to the pharmaceutical substances most widely applied in concomitant chemoradiotherapy [2]. Besides the biological effects of these compounds [3,4], cisplatin and halogenated uracil molecules are also known for their efficiency as radiosensitisers, i.e. they enhance DNA damage and tumour cell killing rates upon irradiation of the targeted cells [5–10]. In contrast, *Gem* has been widely applied in anticancer therapy rather due to its effectiveness towards a broad range of tumours by being highly efficient in inhibiting DNA synthesis and repair [3]. However, it has also been suggested that fluorination of nucleosides results in increased induction of DNA damage via fragmentation due to enhancement of the electron attachment process [11]. Fragmentation enhancement factors of 2.8–5.5 have been reported depending on the location of fluorination in 2′-deoxycytidine (denoted simply as *Cyt* for the remainder of this work) suggesting *Gem* also as an efficient radiosensitiser [11].

Generally, when biological tissue is irradiated, products of ionising radiation such as electrons not only interact with the biomolecular environment but also with administered pharmaceuticals. Among others, such as electron attachment processes, electron impact ionisation processes constitute dominant processes for electron molecule scattering phenomena and play also a role in interatomic Coulombic decay (ICD) which is driven by energy transfer [12]. Upon ICD, an ionised compound relaxes via transferring its excess energy to a neighbouring molecule which then becomes also ionised, resulting finally in two positively charged products that repel each other and subsequently often break apart [13]. ICD represents one of the processes which need to be considered especially in the context of electron interaction with molecules in biological environments. Data on the probability distribution characterising the interaction of the ionising radiation with the cell as a function of impact energy are then required as input for modelling purposes using e.g. Monte-Carlo track structure simulations [14,15]. In general, these simulations also require, among other input, single and double differential cross sections (SDCSs and DDCSs) to properly describe the effects of secondary electrons in media. For total cross sections, which can sometimes be enough for some purposes, two widely established methods are the Deutsch-Märk (DM) method [16], see Section 2.1, as well

* Contribution to the Topical Issue "Dynamics of Systems on the Nanoscale (2018)", edited by Ilko Bald, Ilia A. Solov'yov, Nigel J. Mason and Andrey V. Solov'yov.

[a] e-mail: s.huber@uibk.ac.at
[b] e-mail: andreas.mauracher@uibk.ac.at

as the binary-encounter-Bethe (BEB) method [17,18], see Section 2.2. While the DM method does not offer a possibility to calculate differential cross sections, the BEB method allows in principle to derive SDCSs (energy distributions) although their shapes may not be realistic [17]. To arrive at more realistic SDCSs in the framework of inelastic electron scattering, the more sophisticated binary-encounter-dipole method can be employed. The modified Jain-Khare semi-empirical approach is the only method that can be used to calculate (partial) SDCSs and DDCSs for molecules in electron ionisation [19]. In the context of radiation damage of biological tissue, interaction of ionising particles with condensed matter is also of importance. For such systems, methods exist which combine a relative simplicity, accuracy and generality, which can provide both total and differential ionisation cross sections. Many of those are based on the dielectric formalism, which are applicable for ions [20–22] and electron impact [23–25]. Although it is important to note that many ingredients are typically necessary as input for the mentioned Monte-Carlo track simulations, we focus here on a subset of these, i.e. the total cross sections. In particular, we choose the above mentioned DM and BEB methods to compute (total) electron-impact ionisation cross sections (EICSs) due to the typical reliability, simplicity and generality of these models, see also below.

Here, we assess calculated EICSs for the molecules *Cyt*, *Gem* and 2′-deoxy-5-fluorocytidine (*fCyt* for the reminder of this work), see Figure 1. These molecules also represent building blocks of larger (fluorinated) DNA sequences. In order to investigate effects due to different direct biomolecular environments on the resulting EICSs, we report and compare thus also the cross sections of the sequences *Cyt-Cyt*, *fCyt-Cyt*, *Cyt-fCyt*, *Gem-Cyt* and *Cyt-Gem* (written in a 3′-to-5′ direction). These sequences are constructed as illustrated in Figure 1 for the case of *Gem-Cyt*. Moreover, we report also EICSs for the considered molecules when they are embedded in an aqueous solvent.

The distribution of the energies of secondary electrons, i.e. electrons produced by highly-energetic primary ionising radiation, has its maximum typically in the range of a few tens of eV ($=1.602\times10^{-19}$ J) beyond which it decreases up to primary impact energies of about 10 keV [26]. We hence calculate EICSs in an energy range from threshold to 10 keV. Furthermore, we compare two of the most-widely used methods for the computation of EICSs, i.e. the BEB theory of Kim et al. [17,18] and the DM method [16]. Both types of methods have been successfully applied to atoms, molecules, clusters, ions and radicals. Their accuracy is typically in the same range as the one of experimental data [27].

2 Methods

2.1 The Deutsch-Märk (DM) method

The DM method was originally developed as an easy-to-use, semi-empirical approach for the calculation of EICSs of atoms in their electronic ground state from threshold

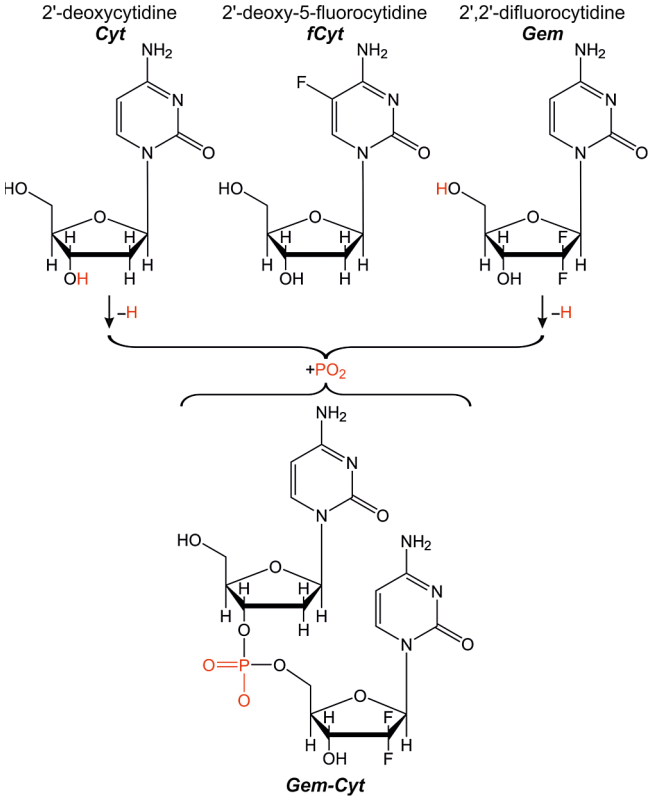

Fig. 1. Schematics of the structures of the considered (fluorinated) nucleosides *Cyt*, *fCyt* and *Gem* (top) and illustration of how the sequence *Gem-Cyt* was constructed from its constituents (bottom).

to about 100 eV [16]. In a more recent variant of the DM method [27,28], the total single electron-impact ionisation cross section σ_{DM} of an atom is expressed as:

$$\sigma_{\mathrm{DM}}(u)=\sum_{n,l} g_{nl}\pi r_{nl}^2\xi_{nl}b_{nl}^{(\xi_{nl})}(u)\left[\ln\left(c_{nl}u\right)/u\right], \qquad (1)$$

where r_{nl} is the radius of maximum radial density of the atomic sub-shell characterised by quantum numbers n and l (as listed in column 1 in the tables of Desclaux [29]) and ξ_{nl} is the number of electrons in that sub-shell. The sum extends over all atomic sub-shells labelled by n and l. The g_{nl} are weighting factors, that were originally introduced by Bethe as a function of the quantum numbers n and l using hydrogenic wave functions [30]. A historical description of their use in the DM method is given in reference [32]. More particularly, they were originally determined by a fitting procedure [31,32] using reliable experimental cross section data for a few selected atoms, for which the accuracy of the reported rate is in the range of 7−15%. The reduced energy u is given by $u=E/E_{nl}$, where E refers to the incident energy of the electrons and E_{nl} denotes the ionisation energy of the sub-shell characterised by n and l. The energy-dependent quantities $b_{nl}^{(\xi_{nl})}(u)$ were introduced in an effort to merge the high-energy region of the ionisation cross section, which follows the Born-Bethe approximation [30], with the DM formula

of the cross sections in the regime of low impact energies. The function $b_{nl}^{(\xi_{nl})}$ in equation (1) has the explicit form:

$$b_{nl}^{(\xi_{nl})} = \frac{A_1 - A_2}{1 + (u/A_3)^p} + A_2. \quad (2)$$

The four constants A_1, A_2, A_3 and p were determined, together with c_{nl}, from reliably measured cross sections for the various values of n and l [32]. The superscript ξ_{nl} in equation (2) was introduced to allow the possibility to use slightly different functions $b_{nl}^{(\xi_{nl})}$ depending on the number of electrons in the respective sub-shell. At high impact energies u goes to infinity, the first term in equation (2) goes to zero and $b_{nl}^{(\xi_{nl})}(u)$ becomes a constant ensuring the high-energy dependence of the cross sections predicted by the Born-Bethe theory [30].

The DM formalism has been extended to the calculation of EICSs of atoms in excited states, molecules and free radicals, atomic and molecular ions, and clusters [27]. For the calculation of the EICS of a molecule, a population analysis [33,34] must be carried out to obtain the weights with which the atomic orbitals of the constituent atoms contribute to each occupied molecular orbital. These weights are obtained from the coefficients of the occupied molecular orbital after a transformation employing the overlap matrix in order to correct for the non-orthogonality of the atomic basis functions.

2.2 The binary-encounter-Bethe (BEB) method

The BEB model [18] was derived from the binary-encounter-dipole model [17] by replacing the $\mathrm{d}f/\mathrm{d}E$ term for the continuum dipole oscillator strengths by a simpler form. Thus, a modified form of the Mott cross section together with the asymptotic form of the Bethe theory describing the electron-impact ionisation of an atom was combined into an expression for the cross section:

$$\sigma_{\mathrm{BEB}}(t) = \sum_{\mathrm{occ.MOs}} \frac{S}{t+u+1} \times \left[\frac{\ln(t)}{2}\left(1 - \frac{1}{t^2}\right) + 1 - \frac{1}{t} - \frac{\ln(t)}{t+1}\right], \quad (3)$$

where $t = E/B$, $u = U/B$, $S = 4\pi a_0^2 N R^2/B^2$, a_0 denotes the Bohr radius (0.5292 Å), R is the Rydberg energy (13.6057 eV), and E denotes again the incident electron energy. N, B and U are the electron occupation number, the binding energy (ionisation energy), and the average kinetic energy of the respective molecular orbital (MO), respectively. In the BEB model, the total cross section, similarly to the DM method, is then obtained by summation over the cross sections for all occupied MOs as symbolically indicated in equation (3).

2.3 Quantum chemical calculations

After optimising geometries using the Amber99 force field [35], the orbital populations required for the DM formalism were subsequently determined via Hartree-Fock (HF) calculations in conjunction with the minimal CEP-4G basis set [36–38]. Although larger basis sets result in a better quality of the overall wave function, the decomposition into the atomic orbitals contributing to the molecular wave function becomes worse due to the increasing overlap between atomic orbitals centered at different nuclei. Occupation, binding energy and average kinetic energy for each molecular orbital, as required for the calculation of the BEB cross sections, were also calculated at the HF/Def2-TZVP [39] level of theory. In this case, the approximation of the electron binding energy via Koopman's theorem represents a more considerable limitation than the choice of basis set. However, methods yielding typically more accurate estimates for the binding energies such as outer valence Green's function electron propagator theory [40] become computationally easily demanding if not unfeasible (depending of course also on the accessible computational resources). Moreover, all calculations were repeated using the polarizable continuum model (PCM) [41–44] in order to approximate effects due to an aqueous solvent. In the PCM, the interaction between a quantum mechanically described solute and the continuum modelling the solvent is mediated solely by the permittivity of the solvent. To compute the electrostatic potential due to the polarization of the dielectric solvent surrounding the solute, a molecular shaped cavity is generated by interlocking van-der-Waals spheres centered at the locations of the nuclei constituting the molecule. To obtain the molecular electrostatic potential and subsequently the solvation energy, the Poisson problem is solved approximately. For details see e.g. reference [43].

2.4 Analytical expression of the EICSs

We also fitted all cross sections to an analytical 5-parameter expression that has its roots originally in the framework of nuclear fusion research, e.g. for usage in the ERO code [45–47], but allows straightforward implementation and on-line computation of cross sections (instead of supplying them as tabular input) regardless of the specific computational modelling context. The fitting expression is given by:

$$\sigma(E) = \left(\frac{a_1}{E}\right)\left[1 - \frac{E_{\mathrm{th}}}{E}\right]^{a_2}\left[\ln\left(\frac{E}{E_{\mathrm{th}}}\right) + a_3 + a_4\left(\frac{E_{\mathrm{th}}}{E}\right)\right]. \quad (4)$$

Here, the cross section σ is expressed in Å^2 ($=10^{-20}$ m^2), the incident electron energy E and the threshold energy E_{th} (i.e. the first or rather the lowest ionisation energy) are both expressed in eV. The fit parameter a_1 has the unit Å^2 eV while a_2, a_3 and a_4 are dimensionless.

3 Results and discussion

The EICSs for gas-phase *Cyt*, *fCyt* and *Gem* obtained with the DM and BEB methods in the energy range from threshold to 10 keV are depicted in Figure 2. The computed threshold energies, i.e. the first ionisation energies,

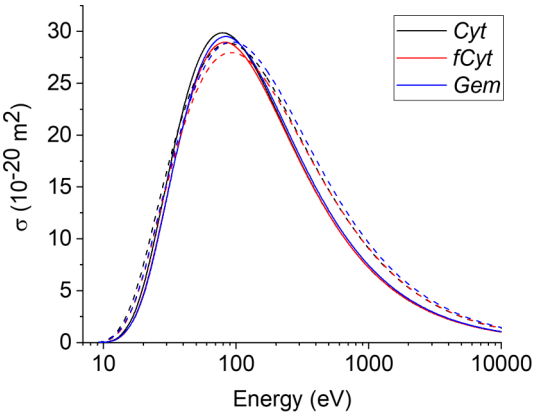

Fig. 2. EICSs for *Cyt* (black lines), *fCyt* (red lines) and *Gem* (blue lines) as obtained with the DM (solid lines) and BEB (dashed lines) methods.

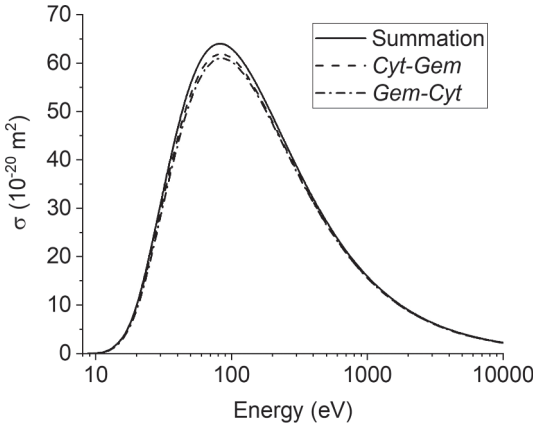

Fig. 3. EICSs obtained with DM for the sequences Cyt-Gem (dashed line) and Gem-Cyt (dash-dotted line). The cross section obtained by summing the cross sections of the molecular constituents of the sequences (as explained in the text) is given by the solid line.

have been 9.04 eV, 9.11 eV and 9.16 eV for *Cyt*, *fCyt* and *Gem*, respectively. Hence, fluorination affects the ionisation energy only slightly. An experimental value for the ionisation energy of *Cyt* yields 8.46 eV [48] in reasonable agreement with the value determined by Koopman's theorem. The DM cross sections yield maxima of 29.88 Å^2 at 79 eV, 28.96 Å^2 at 82.2 eV and 29.51 Å^2 at 83.4 eV for *Cyt*, *fCyt* and *Gem*, respectively. The BEB cross sections yield maxima of 28.89 Å^2 at 87.6 eV, 27.97 Å^2 at 91.6 eV and 29.02 Å^2 at 93.4 eV for *Cyt*, *fCyt* and *Gem*, respectively. Hence, we find excellent agreement between the DM and BEB methods, within about 3−4% at the cross section maxima. The DM cross sections yield a somewhat smoother increase in the threshold region, followed by a steeper increase towards the maximum and also a steeper decrease after reaching their maximum compared to the BEB cross sections which appears as a typical feature when comparing results obtained with the two methods, see e.g. references [49–52].

The molecules considered in this work can be viewed as building blocks of larger (fluorinated DNA) sequences. It has been found that the specifics of the sequence at hand can influence resulting outcomes such as the number of electron-induced DNA strand breaks [53–55]. Here, we investigated (to some extent) how the EICSs are influenced if larger nucleotide units are built from the three bare nucleosides under consideration. In particular, we computed the EICSs of the sequences *Cyt-Cyt*, *fCyt-Cyt*, *Cyt-fCyt*, *Gem-Cyt* and *Cyt-Gem*. The DM cross sections for these sequences yield maxima of 62.48 Å^2 at 81 eV, 61.75 Å^2 at 82.8 eV, 61.92 Å^2 at 82.4 eV, 61.02 Å^2 at 84.4 eV and 61.93 Å^2 at 83.2 eV, respectively. The BEB cross sections yield maxima of 60.61 Å^2 at 89.2 eV, 60.23 Å^2 at 91.0 eV, 60.54 Å^2 at 90.8 eV, 59.02 Å^2 at 93 eV and 60.34 Å^2 at 92.2 eV, respectively. Hence, the two methods again yield excellent agreement with each other, within 2−3%. The threshold energies (first ionisation energies) have been computed to 8.68 eV, 8.76 eV, 9.02 eV, 8.80 eV and 8.86 eV, respectively.

In a first approximation, cross sections for larger molecular compounds can to some extent be estimated by summation of the cross sections of their individual parts. This approach was followed sometimes in earlier work to estimate molecular cross sections from known atomic cross sections [56–58] which yields at least an upper bound for the real molecular cross sections. Improving the approximation, however, requires a refined approach [59].

Here, we investigate how well the cross sections of the considered sequences are approximated by adding the cross sections of their building blocks. In particular, we approximate the cross section of the sequence $X-Y$ by

$$\sigma^{(\text{approx.})}(X-Y) \approx \sigma(X) + \sigma(Y) + \sigma(PO_2) - 2\times\sigma(H), \quad (5)$$

with $X-Y =$ *Cyt-Cyt*, *fCyt-Cyt*, *Cyt-fCyt*, *Gem-Cyt* or *Cyt-Gem*.

In Figure 3, we depict the EICSs obtained with the DM method for the sequences *Gem-Cyt* and *Cyt-Gem* and the cross sections obtained via summation of the individual constituents. Obviously, the cross sections obtained via summation are the same for both sequences. Due to the excellent agreement found between the cross sections obtained with the DM and BEB methods, we limit the following discussion to the case of DM cross sections. We find only a slight influence of the sequence of the constituents for the resulting cross sections. In particular, the EICS for *Gem-Cyt* is slightly smaller by about 1.2 Å^2 than the EICS for *Cyt-Gem*. Moreover, both cross sections are slightly smaller than the approximation via summation which hence, expectedly forms an upper bound for both cross sections. The latter is true only at energies for which each of the summed terms in equation (5) yields non-zero values. Otherwise, it may happen that the cross section of the compound system is smaller than the one obtained by summation simply because the ionisation threshold of the compound is smaller than the ones of the constituents. This is seen also in Figure 4, in which we plot the differences between DM cross sections of the considered sequences and the approximations obtained via summation, i.e. $\Delta\sigma = \sigma^{(\text{DM})} - \sigma^{(\text{approx.})}$. Apart from this feature in the threshold region, we note that absolute differences between the compared cross sections are below 3.5 Å^2 for

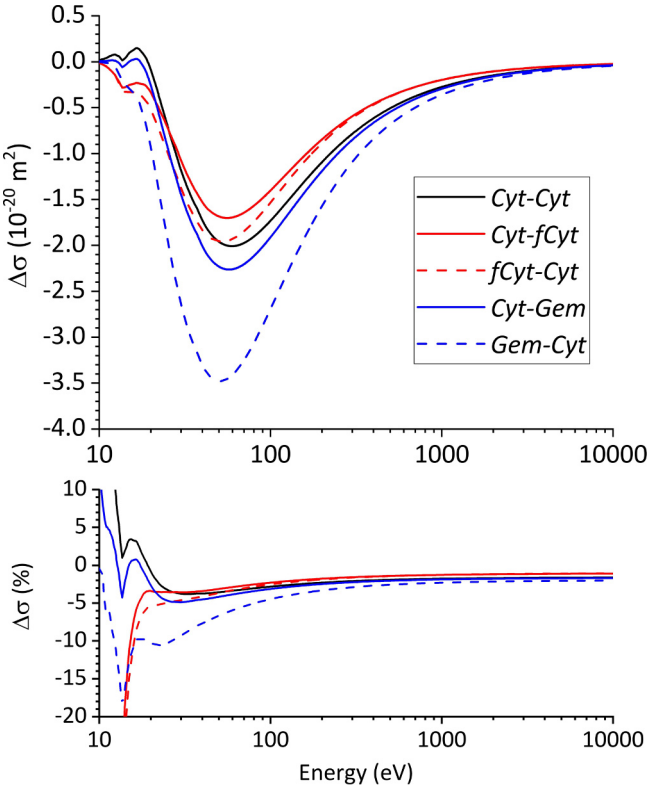

Fig. 4. Differences (absolute: top panel; relative: bottom panel) between EICSs computed for all considered sequences and the corresponding approximations via summation of EICSs of the constituting molecular parts as described in the text.

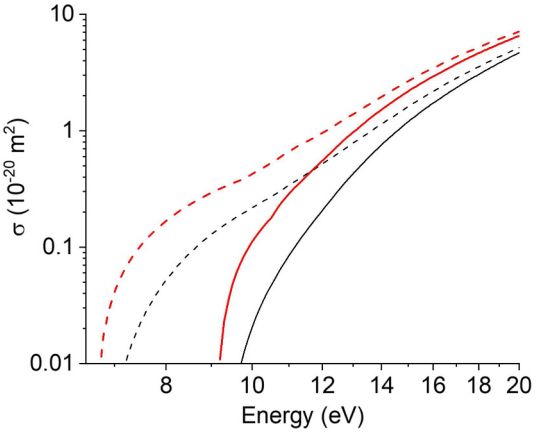

Fig. 5. EICSs obtained with the DM (black lines) and BEB (red lines) methods for *fCyt* in the gas-phase (solid lines) and applying the PCM with an aqueous solvent (dashed lines) in the energy range from 6.5 to 20 eV.

all sequences under consideration which accounts for a relative agreement within about 6% at the cross section maxima and beyond (see Fig. 4). Hence, the cross sections for the considered sequences and supposedly also the ones for larger sequences may be approximated rather well by summation of cross sections of their individual molecular parts although subtle differences with respect to the relative order of constituents in the sequences is obviously lost then.

Solvent effects may affect the ionisation thresholds quite substantially which then, as a consequence affect also the resulting EICSs. For the considered bare nucleosides *Cyt*, *fCyt* and *Gem* we obtain 9.40 eV, 6.65 eV and 9.55 eV, respectively, when using the PCM to model effects of an aqueous environment. Earlier experimental and theoretical investigations yield an ionisation energy of *Cyt* in aqueous solution of 8.3 eV and 7.8 eV [48], respectively, which are considerably lower values than the ones obtained by us. We note thus, that our computational model may overestimate the resulting ionisation energies which, however, puts even more emphasis on the following discussion.

Whereas for *Cyt* and *Gem* the obtained threshold numbers are quite comparable to the gas-phase (for which they have been 9.04 eV and 9.16 eV, respectively), for *fCyt* the ionisation threshold is lowered by about 2.5 eV due to the aqueous solvent. For the considered sequences *Cyt-Cyt*, *fCyt-Cyt*, *Cyt-fCyt*, *Gem-Cyt* and *Cyt-Gem* we obtain ionisation thresholds of 7.56 eV, 9.55 eV, 9.51 eV, 9.42 eV and 9.54 eV, respectively, using the PCM compared to 8.68 eV, 8.76 eV, 9.02 eV, 8.80 eV and 8.86 eV, respectively, in the gas-phase, giving rise to changes in the ionisation energy in a range from 0.49 to 1.12 eV.

These changes in ionisation energy affect also the resulting ionisation cross sections mostly in the energy region close to the threshold, which is illustrated for the most extreme case, i.e. the fluorinated nucleoside *fCyt*, in Figure 5. There we plot the EICSs obtained with the DM and BEB methods for this molecule on a double-logarithmic scale. We find that, in an aqueous environment ionisation processes can be more abundant by an order of magnitude than in the gas phase for electron energies of about 10 eV close to the ionisation thresholds due to the considerably larger ionisation cross section, see Figure 5. However, we note that although ionisation is typically more likely in a polar solvent, we also obtained ionisation thresholds considerably larger when employing the PCM than in the gas phase (see Tab. 1). Some of the variation in our results cannot be excluded to be due to approximating the ionisation thresholds using Koopman's theorem. Hence, what may be safely stated, is rather that solvation *can* have a considerable effect also on electron impact ionisation and associated processes. Especially in the framework of fundamental research on the interaction of radiation with biological matter such as in radiochemotherapy, the importance of secondary low-energy electrons as mediators for DNA damage is well-established [60–63]. Furthermore, it has become well-known that the aqueous environment typically present in biological tissue can have substantial effects on a variety of molecular properties and processes [64]. In this respect, our findings put further emphasis on the need to be cautious with the interpretation and even more so with the eventual generalisation of either experimentally or computationally obtained results in the gas-phase. Nevertheless, it has become clear that in principle solvation *can* substantially affect electron impact ionization.

For completeness, we supply also the cross section maxima and their locations (at the energy-scale) of the various considered molecules in the case of applying the PCM in order to characterise the respective cross sections. For

Table 1. Computed ionisation thresholds and fit coefficients as obtained with the DM and BEB methods as well as with the gas-phase and polarisable continuum models for all molecules considered in this work.

Molecule	Model	E_{th} (eV)	a_1 (Å^{2}eV)		a_2		a_3		a_4	
			DM	BEB	DM	BEB	DM	BEB	DM	BEB
Cyt	Gas-phase	9.04	1223	2493	5.663	4.177	1.642	−0.8544	0.238	1.797
	PCM	9.40	1249	2460	5.359	4.067	1.554	−0.8193	0.0382	1.763
fCyt	Gas-phase	9.11	1245	2519	5.811	4.472	1.568	−0.8737	0.08217	1.944
	PCM	6.65	1122	2400	8.778	7.331	1.9	−0.9647	0.3141	3.098
Gem	Gas-phase	9.16	1292	2694	5.867	4.42	1.542	−0.9231	0.09874	1.953
	PCM	9.55	1295	2657	5.638	4.287	1.554	−0.8864	0.05936	1.911
Cyt-Cyt	Gas-phase	8.68	2636	5287	6.068	4.624	1.567	−0.8772	0.15	1.983
	PCM	7.56	2343	4954	7.7	6.658	2.133	−0.8149	0.3854	3.084
Cyt-fCyt	Gas-phase	9.02	2657	5414	5.946	4.458	1.592	−0.8816	0.1528	1.951
	PCM	9.51	2713	5319	5.564	4.348	1.518	−0.8326	0.1084	1.937
fCyt-Cyt	Gas-phase	8.76	2602	5348	6.256	4.76	1.688	−0.8772	0.1646	2.062
	PCM	9.55	2716	5321	5.537	4.319	1.51	−0.8314	0.1075	1.925
Cyt-Gem	Gas-phase	8.86	2689	5474	6.125	4.677	1.559	−0.9034	0.1463	2.037
	PCM	9.55	2737	5424	5.626	4.373	1.515	−0.853	0.1205	1.955
Gem-Cyt	Gas-phase	8.80	2644	5354	6.324	4.887	1.629	−0.887	0.1478	2.104
	PCM	9.42	2712	5385	5.753	4.527	1.545	−0.8474	0.1297	2.019

the bare nucleosides *Cyt*, *fCyt* and *Gem*, the DM cross sections yield maxima of 29.61 Å^2 at 79.6 eV, 28.94 Å^2 at 82 eV and 29.2 Å^2 at 84.2 eV, respectively. The BEB cross sections for these molecules yield maxima of 28.30 Å^2 at 88.4 eV, 28.33 Å^2 at 90.6 eV and 28.42 Å^2 at 94.2 eV, respectively. For the considered sequences *Cyt-Cyt*, *fCyt-Cyt*, *Cyt-fCyt*, *Gem-Cyt* and *Cyt-Gem*, the DM cross sections yield maxima of 61.74 Å^2 at 81.8 eV, 61.38 Å^2 at 83.2 eV, 61.48 Å^2 at 83 eV, 61.09 Å^2 at 84.4 eV and 61.28 Å^2 at 84.2 eV, respectively. The BEB cross sections for these molecules yield maxima of 58.83 Å^2 at 90.8 eV, 58.78 Å^2 at 92.2 eV, 58.81 Å^2 at 92 eV, 58.69 Å^2 at 93.6 eV and 58.89 Å^2 at 93.4 eV, respectively. Comparison of these values with respective gas-phase results shows that the cross section maxima are largely unaffected by effects of an aqueous solvent. The same holds for elevated energies beyond the maxima. Hence, solvent effects are of most importance especially for low impact energies around the ionisation thresholds.

In Table 1, we summarise all ionisation thresholds for all considered molecules in both cases, i.e. in gas-phase and in aqueous solution. We also supply the obtained fit coefficients for fitting the computed cross sections to the analytical 5-parameter expression described in Section 2.4.

4 Conclusions

We computed electron-impact ionisation cross sections (EICSs) for 2′-deoxycytidine (*Cyt*) and two fluorinated variants of this nucleoside, 2′-deoxy-5-fluorocytidine (*fCyt*) and 2′,2′-difluorocytidine (gemcitabine, *Gem*). We compared the Deutsch-Märk (DM) and the binary-encounter-Bethe (BEB) methods to obtain these cross sections. The DM cross sections for *Cyt*, *fCyt* and *Gem* yield maxima of 29.88 Å^2 at 79 eV, 28.96 Å^2 at 82.2 eV and 29.51 Å^2 at 83.4 eV, respectively, whereas the BEB cross sections yield maxima of 28.89 Å^2 at 87.6 eV, 27.97 Å^2 at 91.6 eV and 29.02 Å^2 at 93.4 eV, respectively. The two methods are thus in excellent agreement with each other, within 3−4% at the cross section maxima. We found further that EICSs for the small nucleotide sequences *Cyt-Cyt*, *fCyt-Cyt*, *Cyt-fCyt*, *Gem-Cyt* and *Cyt-Gem*, are only slightly affected by the order of the constituents of the sequence and can be approximated with an accuracy within 6% by simply adding the EICSs of individual molecular constituents. In addition, we computed EICSs applying the polarisable continuum model (PCM) to study eventual effects of an aqueous environment. We found that differences in the ionisation energy due to the aqueous solvent can be substantial and hence, affect also the EICSs especially around the threshold region. This puts further emphasis on exercising caution when interpreting results obtained in the gas-phase in the framework of research on the interaction of radiation and particularly secondary low-energy electrons with biological matter. Finally, we fitted all computed EICSs to an analytical 5-parameter expression in order to allow straightforward implementation and usage in further computational research.

Open access funding provided by Austrian Science Fund (FWF). This work was supported by the Austrian Ministry of Science BMWF as part of the University infrastructure program of the scientific computing platform LFU Innsbruck. This work was supported by the Austrian Fund Agency (FWF, P 30355).

Author contribution statement

All authors contributed equally to the paper.

References

1. L. Pecorino, *Molecular biology of cancer* (Oxford University Press, Oxford, 2016)
2. T.Y. Seiwert, J.K. Salama, E.E. Vokes, Nat. Clin. Pract. Oncol. **4**, 156 (2007)
3. G.D. Wilson, S.M. Bentzen, P.M. Harari, Semin. Radiat. Oncol. **16**, 2 (2006)
4. D.S. Shewach, T.S. Lawrence, J. Clin. Oncol. **25**, 4043 (2007)
5. H. Abdoul-Carime, M.A. Huels, E. Illenberger, L. Sanche, J. Am. Chem. Soc. **123**, 5354 (2001)
6. M. Rezaee, D.J. Hunting, L. Sanche, Int. J. Radiat. Oncol. Biol. Phys. **87**, 847 (2013)
7. J. Kopyra, C. Koenig-Lehmann, I. Bald, E. Illenberger, Angew. Chem. Int. Ed. **48**, 7904 (2009)
8. J. Reedijk, Eur. J. Inorg. Chem. **2009**, 1303 (2009)
9. S. Denifl, P. Candori, S. Ptasinska, P. Limao-Vieira, V. Grill, T. D. Märk, P. Scheier, Eur. Phys. J. D **35**, 391 (2005)
10. Y. Park, K. Polska, J. Rak, J.R. Wagner, L. Sanche, J. Phys. Chem. B **116**, 9676 (2012)
11. J. Kopyra, A. Keller, I. Bald, RSC Adv. **4**, 6825 (2014)
12. X.G. Ren, E.J. Al Maalouf, A. Dorn, S. Denifl, Nat. Commun. **7**, 11093 (2016)
13. L.S. Cederbaum, J. Zobeley, F. Tarantelli, Phys. Rev. Lett. **79**, 4778 (1997)
14. M. Dingfelder, Radiat. Prot. Dosim. **122**, 16 (2006)
15. M. Müller, M. Durante, H. Stocker, F. Merz, I. Bechmann, Eur. Phys. J. D **60**, 171 (2010)
16. H. Deutsch, T.D. Märk, Int. J. Mass Spectrom. **79**, R1 (1987)
17. Y.K. Kim, M.E. Rudd, Phys. Rev. A **50**, 3954 (1994)
18. Y.K. Kim, M.A. Ali, M.E. Rudd, J. Res. Nat. Inst. Stand. Technol. **102**, 693 (1997)
19. S.P. Khare, S. Prakash, W.J. Meath, Int. J. Mass Spectrom. Ion Processes **88**, 299 (1989)
20. M. Dingfelder, Radiat. Prot. Dosim. **99**, 23 (2002)
21. P. de Vera, R. Garcia-Molina, I. Abril, A. V. Solov'yov, Phys. Rev. Lett. **110**, 148104 (2013)
22. P. de Vera, R. Garcia-Molina, I. Abril, Phys. Rev. Lett. **114**, 018101 (2015)
23. D. Emfietzoglou, H. Nikjoo, Radiat. Res. **163**, 98 (2005)
24. D. Emfietzoglou, H. Nikjoo, Radiat. Res. **167**, 110 (2007)
25. D. Emfietzoglou, G. Papamichael, H. Nikjoo, Radiat. Res. **188**, 355 (2017)
26. S.M. Pimblott, J.A. LaVerne, Radiat. Phys. Chem. **76**, 1244 (2007)
27. H. Deutsch, K. Becker, M. Probst, T.D. Märk, in *Advances in atomic, molecular, and optical physics*, edited by E. Arimondo, P. R. Berman, C.C. Lin (Elsevier Academic Press Inc, San Diego, 2009), Vol. 57
28. H. Deutsch, P. Scheier, K. Becker, T.D. Märk, Int. J. Mass Spectrom. **233**, 13 (2004)
29. J.P. Desclaux, At. Data Nucl. Data Tables **12**, 311 (1973)
30. H. Bethe, Ann. Phys. **397**, 325 (1930)
31. D. Margreiter, H. Deutsch, T.D. Märk, Int. J. Mass Spectrom. Ion Processes **139**, 127 (1994)
32. H. Deutsch, K. Becker, S. Matt, T.D. Märk, Int. J. Mass Spectrom. **197**, 37 (2000)
33. R.S. Mulliken, J. Chem. Phys. **23**, 1833 (1955)
34. R. Tang, J. Callaway, J. Chem. Phys. **84**, 6854 (1986)
35. J. Wang, P. Cieplak, P.A. Kollman, J. Comput. Chem. **21**, 1049 (2000)
36. W.J. Stevens, H. Basch, M. Krauss, J. Chem. Phys. **81**, 6026 (1984)
37. W.J. Stevens, M. Krauss, H. Basch, P.G. Jasien, Can. J. Chem. **70**, 612 (1992)
38. T.R. Cundari, W.J. Stevens, J. Chem. Phys. **98**, 5555 (1993)
39. F. Weigend, R. Ahlrichs, Phys. Chem. Chem. Phys. **7**, 3297 (2005)
40. W. Von Niessen, J. Schirmer, L. S. Cederbaum, Comput. Phys. Rep. **1**, 57 (1984)
41. M. Cossi, V. Barone, R. Cammi, J. Tomasi, Chem. Phys. Lett. **255**, 327 (1996)
42. V. Barone, M. Cossi, J. Tomasi, J. Chem. Phys. **107**, 3210 (1997)
43. J. Tomasi, B. Mennucci, R. Cammi, Chem. Rev. **105**, 2999 (2005)
44. S. Miertus, E. Scrocco, J. Tomasi, Chem. Phys. **55**, 117 (1981)
45. D. Naujoks, R. Behrisch, J.P. Coad, L. Dekock, Nucl. Fusion **33**, 581 (1993)
46. A. Kirschner, V. Philipps, J. Winter, U. Kogler, Nucl. Fusion **40**, 989 (2000)
47. D. Borodin, A. Kirschner, S. Carpentier-Chouchana, R.A. Pitts, S. Lisgo, C. Björkas, P.C. Stangeby, J.D. Elder, A. Galonska, D. Matveev, V. Philipps, U. Samm, Phys. Scr. **T145**, 014008 (2011)
48. P. Slavíček, B. Winter, M. Faubel, S.E. Bradforth, P. Jungwirth, J. Am. Chem. Soc. **131**, 6460 (2009)
49. I. Sukuba, A. Kaiser, S.E. Huber, J. Urban, M. Probst, Eur. Phys. J. D **70**, 11 (2016)
50. S.E. Huber, I. Sukuba, J. Urban, J. Limtrakul, M. Probst, Eur. Phys. J. D **70**, 182 (2016)
51. S.E. Huber, D. Süß, M. Probst, A. Mauracher, Mol. Phys. (2018) DOI: 10.1080/00268976.2018.1509148
52. S.E. Huber, A. Mauracher, D. Süß, I. Sukuba, J. Urban, D. Borodin, M. Probst, J. Chem. Phys. **150**, 024306 (2019)
53. A. Keller, J. Rackwitz, E. Cauët, J. Liévin, T. Körzdörfer, A. Rotaru, K.V. Gothelf, F. Besenbacher, I. Bald, Sci. Rep. **4**, 7391 (2014)
54. J. Rackwitz, M.L. Ranković, A.R. Milsavljević, I. Bald, Eur. Phys. J. D **71**, 32 (2017)
55. J. Rackwitz, I. Bald, Chem. Eur. J. **24**, 4680 (2018)
56. K.L. Baluja, A. Agrawal, Phys. Lett. A **198**, 225 (1995)
57. T.D. Märk, G.H. Dunn, *Electron impact ionization* (Springer, Wien, 1985)
58. S.E. Huber, A. Mauracher, I. Sukuba, J. Urban, T. Maihom, M. Probst, Eur. Phys. J. D **71**, 335 (2017)
59. H. Deutsch, K. Becker, T.D. Märk, Int. J. Mass Spectrom. **167**, 503 (1997)
60. Z. Li, P. Cloutier, L. Sanche, J.R. Wagner, J. Am. Chem. Soc. **132**, 5422 (2010)
61. M. McAllister, M. Smyth, B. Gu, G.A. Tribello, J. Kohanoff, J. Phys. Chem. Lett. **6**, 3091 (2015)
62. L. Sanche, Radiat. Phys. Chem. **128**, 36 (2016)
63. K. Jorge, M. Maeve, A.T. Gareth, G. Bin, J. Phys.: Condens. Matter **29**, 383001 (2017)
64. J.D. Gu, J. Leszczynski, H.F. Schaefer, Chem. Rev. **112**, 5603 (2012)